JOURNAL OF VIROLOGY, Dec. 1997, p. 9844–9848 Vol. 71, No. 12
0022-538X/97/$04.00+0

A Decay-Accelerating Factor-Binding Strain of Coxsackievirus B3 Requires the Coxsackievirus-Adenovirus Receptor Protein To Mediate Lytic Infection of Rhabdomyosarcoma Cells

DARREN R. SHAFREN,* DAVID T. WILLIAMS,† AND RICHARD D. BARRY

Department of Microbiology, Faculty of Medicine, The University of Newcastle, Newcastle 2300, Australia

Received 24 April 1997/Accepted 20 August 1997

The composition of the cellular receptor complex for coxsackievirus B3 (CVB3) has been an area of much contention for the last 30 years. Recently, two individual components of a putative CVB3 cellular receptor complex have been identified as (i) decay-accelerating factor (DAF) and (ii) the coxsackievirus-adenovirus receptor protein (CAR). The present study elucidates the individual roles of DAF and CAR in cell entry of CVB3 Nancy. First, we confirm that the DAF-binding phenotype of CVB3 correlates to the presence of key amino acids located in the viral capsid protein, VP2. Second, using antibody blockade, we show that complete protection of permissive cells from infection by high input multiplicities of CVB3 requires a combination of both anti-DAF and anti-CAR antibodies. Finally, it is shown that expression of the CAR protein on the surface of nonpermissive DAF-expressing RD cells renders them highly susceptible to CVB3-mediated lytic infection. Therefore, although the majority of CVB3 Nancy attaches to the cell via DAF, only virus directly interacting with the CAR protein mediates lytic infection. The role of DAF in CVB3 cell infection may be analogous to that recently described for coxsackievirus A21 (D. R. Shafren, D. J. Dorahy, R. A. Ingham, G. F. Burns, and R. D. Barry, J. Virol. 71:4736–4743, 1997), in that DAF may act as a CVB3 sequestration site, enhancing viral presentation to the functional CAR protein.

Coxsackievirus B3 (CVB3) is one of the major causal agents of virus-induced myocarditis. Investigation into the characterization of the CVB3 cell attachment and entry mechanism has been ongoing for the last 30 years, and more recently has become an area of much contention. The key tool used in the identification of the CVB3 cellular receptor has been monoclonal antibody (MAb) blockade of viral binding and replication. Two MAbs (RmcA [9] and RmcB [12]) generated against HeLa cell surface proteins of 70 and 49 kDa, respectively, recognized these proteins to be separate CVB3 receptors. Additionally, RmcA blocked infection by CVB1, CVB3, and CVB5 (9) while RmcB blocked the replication of all six B-group coxsackieviruses (CVBs) (12).

Many CVBs have been shown to replicate poorly or not at all in human diploid fibroblasts and rhabdomyosarcoma (RD) cells (22). Serial blind passage of a Nancy strain of CVB3 in RD cells, however, yielded a variant that induced lytic infection of RD cells and hemagglutinated human erythrocytes (the CVB3 RD variant) (21). This variant agglutinates erythrocytes because it binds to the complement regulatory protein, decay-accelerating factor (DAF) (2), which is highly expressed on the surface of erythrocytes and also on cells that are in contact with serum (20). Consequently, it was postulated that DAF was the functional receptor on RD cells used by the CVB3 RD variant. Since the parental CVB3 from which the RD variant was derived did not bind to DAF nor replicate in RD cells (2), it seemed unlikely that DAF would play a role as a significant receptor for CVB3. Our experience differs, however, in that we find prototype strains of CVB1, CVB3, and CVB5 that have never been passaged in RD cells have DAF-binding affinity (23) and their replication can be inhibited significantly by DAF MAb blockade. Murine cells expressing transfected human DAF can bind these CVBs, although they are refractile to lytic infection (23).

To further complicate matters, it has been reported that a 100-kDa nucleolin-like protein is also likely to be an additional putative receptor for all CVBs (10). This protein induced CVB3 capsid conformational changes and was not a dimer of the previously postulated 49-kDa receptor (12). In addition to the 100-kDa protein, CVB3 was also found to bind to HeLa cell polypeptides with molecular masses of 75 and 50 kDa (10).

More recently the cDNA encoding the surface glycoprotein recognized by MAb RmcB has been cloned and named the coxsackievirus-adenovirus receptor (CAR) (3, 26). CAR is a 46-kDa glycoprotein predicted to have two extracellular immunoglobulin-like domains, a transmembrane domain, and a cytoplasmic tail. Transfection of normally nonpermissive Chinese hamster ovary (CHO) cells with CAR conferred susceptibility to infection by all CVBs (3). CAR also functions as an attachment receptor for adenovirus type 2 (3), which is consistent with an earlier report demonstrating competition for receptor binding sites between CVB3 and adenovirus type 2 (18).

In this study we confirm that the CVB3 DAF-binding phenotype correlates with the presence of a key epitope(s) located in the capsid protein, VP2. We show that antibody-mediated protection of permissive cell lines to high input multiplicities of CVB3 requires the presence of MAbs to both DAF and CAR, since neither MAb alone provided complete protection against viral lysis. Using RD cells in which CAR surface expression has been induced as a consequence of multiple high-density cell passages, we also demonstrate that a DAF-binding strain of CVB3 required CAR in order to establish lytic infection in these cells.

* Corresponding author. Mailing address: Discipline of Pathology, Faculty of Medicine, Level 3, David Maddison Clinical Sciences Building, Royal Newcastle Hospital, Newcastle, New South Wales 2300, Australia. Phone: 61 49 23 6158. Fax: 61 49 23 6814. E-mail: dshafren@mail.newcastle.edu.au.

† Present address: CSIRO, Australian Animal Health Laboratory, Geelong, Victoria 3213, Australia.

TABLE 1. Nucleotide sequences of the primers used to amplify the P1 region of CVB3 Nancy/New

Primer (sense)	5′-3′ sequence	Position (nt)
CVB3 P1-A(+)	TGTGGTTCGGCCATGGCTACT	VP3, 2098–2118
CVB3 P1-A(−)	TAGTTCCCCACATACACTGCC	VP1, 3318–3338
CVB3 P1-B(+)	CAGCAAAATGGGGAGCTCAAGTATCAACC	VP4, 735–763
CVB3 P1-B(−)	CAGCACCTGGTGGTGAGTATGCC	VP3, 2133–2155

Nucleotide sequence of a DAF-binding strain of CVB3 Nancy. A previous nucleotide sequence comparison of the P1 regions of a CVB3 RD variant and its parental CVB3 strain revealed the presence of six amino acid replacements (17). The parental CVB3 gained the RD phenotype when the 5′ part of its P1 region (containing the entire VP2) was replaced with the corresponding genomic segment from the CVB3 RD variant (17). The only amino acid (aa) differences observed between the viral genomic segments were that the RD variant contained a Val and a Ser at aa 108 and 151 of VP2 while the parental strain had an Asp and a Thr, respectively, at these positions. Therefore, it was postulated that the presence of Val 108 and Ser 151 of VP2 plays a crucial role in conferring the RD-positive and DAF-binding phenotypes on CVB3 (2, 15, 17). Previously we have shown that our strain of CVB3 Nancy (designated CVB3 Nancy/New) binds to DAF (23). Using PCR, we amplified the cDNA encoding the capsid proteins (P1 region) of CVB3 Nancy/New and compared this sequence to those of the well-characterized non-DAF-binding CVB3 Nancy (2, 16) and DAF-binding CVB3 RD variant strains used previously (2, 17). Viral RNA was isolated and reverse transcribed by using minor modifications of the protocol described by Vuorinen et al. (27). The oligonucleotide primer pairs, similar to those employed by Lindberg et al. (17), that were used in the PCR to amplify the CVB3 Nancy/New cDNA encoding the P1 region are shown in Table 1.

The amplified DNA fragments were sequenced by the dideoxy termination method with dye terminator cycle sequencing and analyzed on an Applied Biosystems 377 prism DNA sequencer. DNA sequence comparisons were performed by clustal analysis with Sequence Navigator version 1.0 (Applied Biosystems, Inc.) and previously published CVB3 sequences obtained from GenBank. The viral capsid amino acid differences among the three strains of CVB3 Nancy are shown in Table 2. Seven amino acid differences were observed between CVB3 Nancy/New and the parental CVB3 (16), and four differences were observed with the CVB3 RD variant (17). As expected, the sequence of the cDNA encoding VP2 of CVB3 Nancy/New revealed the presence of the key amino acids, Val 108 and Ser 151, considered to confer the DAF-binding phenotype. The nucleotide sequences of the P1 regions of three plaque-purified clones of CVB3 Nancy/New were identical (data not shown). To exclude the possibility of PCR-induced sequence error, the sequence of the PCR-amplified P1 region of a full-length infectious CVB3 cDNA clone, pCB3/T7 (14), was also determined. Unexpectedly, sequence analysis of the VP2 region of this viral clone identified two nucleotide (nt) discrepancies with the published sequence (14): nucleotides G and C instead of C and G were observed at nt 1400 and 1401 (data not shown). To confirm that these differences were not induced during PCR amplification, direct sequencing of the P1 region of the pCB3/T7 plasmid was performed. The partial sequence of the pCB3/T7 VP2 region (nt 1388 to 1415) shown in Fig. 1 confirms that nucleotides G and C at positions 1400 and 1401 are correct, thereby coding for a Ser and not a Thr at aa 151 of VP2. The viral RNA used to construct pCB3/T7 was derived from a CVB3 Nancy strain obtained from the American Type Culture Collection (VR-30), and this strain possesses an RD-negative phenotype (17). This finding contradicts the postulate that the presence of Val 108 and Ser 151 of VP2 is sufficient to confer the RD-positive phenotype. Virus generated from pCB3/T7 binds to DAF on the surface of transfected cells, and this attachment can be blocked by anti-DAF SCR3 MAb pretreatment (data not shown). Furthermore, CVB3 Nancy (VR-30) has been shown to bind to DAF on transfected cells (4).

TABLE 2. Amino acid differences among three strains of CVB3 Nancy

Position (nt)	Amino acid in:		
	Nancy (16)	Nancy/New	Nancy RD (17)
VP1			
23	N	T	T
80	E	E	K
VP2			
108	D	V	V
151	T	S	S
VP3			
137	L	P	L
155	V	I	V
184	C	Y	Y
234	E	L	Q

CVB3 does not infect DAF-expressing RD or MRC-5 cells. Next we investigated whether CVB3 Nancy/New could lytically infect either RD cells or a human diploid fibroblast cell line (MRC-5). Flow cytometric analysis indicated that both cell lines lacked the CAR protein but expressed comparable levels of DAF (Fig. 2). Although DAF expression was much lower than that found on permissive HEp-2 and HeLa-B cells (Fig. 3A), there was nevertheless sufficient DAF on RD or MRC-5 cells to allow lytic infection by another well-characterized DAF-binding virus, echovirus type 7 (1, 6, 28) (data not shown). Confluent monolayers of RD and MRC-5 cells in 96-well plates were each refractile to lytic infection by high input multiplicities of CVB3 Nancy/New (10^6 PFU/well) (data not shown). The apparent RD-negative phenotype of CVB3 Nancy/New contradicted the postulate that DAF-binding strains of CVB3 lytically infected RD cells.

MAb blockade of CVB3 lytic infection. The next step in the investigation was to determine the relative efficiencies of anti-

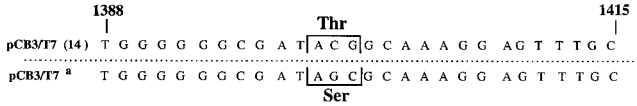

FIG. 1. Partial DNA sequence of the CVB3 cDNA clone, pCB3/T7. The published sequence for pCB3/T7 (14) (nt 1388 to 1415) appears above the sequence of the same cDNA clone (a) that was generated in the present study.

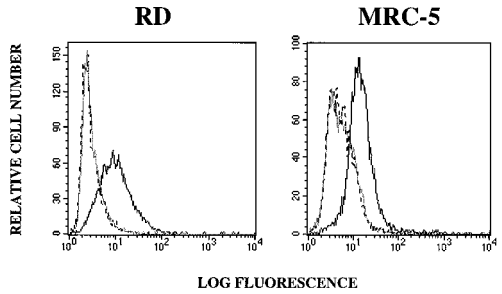

FIG. 2. Relative levels of DAF and CAR expression on RD and MRC-5 cells. Cells (10^6) in 100-μl aliquots were incubated with anti-DAF MAb (IH4) or an anti-CAR MAb (RmcB) diluted in phosphate-buffered saline containing 1% bovine serum albumin (PBS-BSA) on ice for 30 min, after which the cells were washed with 5.0 ml of PBS-BSA. The cells were then pelleted at 1,000 × *g* for 5 min and resuspended in 100 μl of fluorescein isothiocyanate-conjugated goat anti-mouse immunoglobulin G (H+L chains) (Silenus, Melbourne, Australia) diluted in PBS-BSA. Following incubation on ice for 30 min, the cells were washed and pelleted as described above, resuspended in PBS-BSA, and analyzed with a FACStar analyzer (Becton Dickinson, Sydney, Australia). The grey histogram represents binding of the anti-mouse conjugate, the dashed histogram represents binding of the anti-CAR MAb, and the black histogram represents binding of the anti-DAF MAb.

DAF and anti-CAR MAb blockade of CVB3 Nancy/New lytic infection of the permissive cell lines HeLa-B and HEp-2. Flow cytometric analysis of the relative levels of DAF and CAR expressed by the HeLa and HEp-2 cells (Fig. 3A) indicated that both lines expressed comparably high levels of DAF and low levels of CAR, with the HEp-2 cells showing slightly lower levels of expression than the HeLa-B cells. These findings confirm a previous report which indicated that DAF expression was 50-fold greater than that of CAR on the surface of HeLa cells (12). HeLa-B and HEp-2 monolayers in 96-well tissue culture plates were preincubated with anti-DAF MAbs (20 μg/ml) recognizing either DAF SCR1, -2, -3, or -4 (7, 13) prior to challenge with 10^3 PFU of CVB3/well. The data in Fig. 3B show that the anti-DAF SCR3 MAb inhibited the replication of CVB3 in both cell lines. MAbs to DAF SCR1, -2, or -4 had no effect on viral replication.

Similar assays were then carried out with the anti-CAR MAb, RmcB (1/100 dilution of ascites), and as was found with the anti-DAF SCR3 MAb (20 μg/ml), this MAb inhibited viral replication in both cell lines (Fig. 4A and B). The original study of anti-receptor MAb blockade of CVB3 infection used relatively low multiplicities of input virus in the cell protection assays and suggested a possible role for both DAF and CAR in successful lytic infection (12), even though there was no indication of the relative contribution made by each component of the receptor complex. Cell susceptibility to a range of viral input multiplicities under anti-DAF and anti-CAR MAb blockade addresses this question, so experiments were repeated using CVB3 inputs from 1 to 10^6 PFU/well. The results (Fig. 4A) indicated that for both cell lines the anti-CAR MAb blocked lytic infection slightly more effectively at high multiplicity of input virus than the anti-DAF MAb; however, a combination of both MAbs was essential for total blockade of cells challenged at the highest levels of input CVB3.

To determine whether the anti-CAR and anti-DAF MAbs were functioning additively or in synergy, the inhibitory effects of combinations of anti-DAF and anti-CAR MAbs on CVB3 lytic infection were investigated in a dose-dependent manner. Monolayers of HeLa-B cells in 96-well plates were incubated with the anti-DAF SCR3 MAb in concentrations of from 0.625 to 20 μg/ml either alone or in combination with anti-CAR MAb ascites at 1:100, 1:500, or 1:1,000 dilution. Following a 1-h incubation period at 37°C, the cell monolayers were challenged with 10^5 PFU of CVB3. From the results (Fig. 4B) it is clear that the antibodies to DAF and CAR were synergistic in inhibiting CVB3-mediated cell lysis.

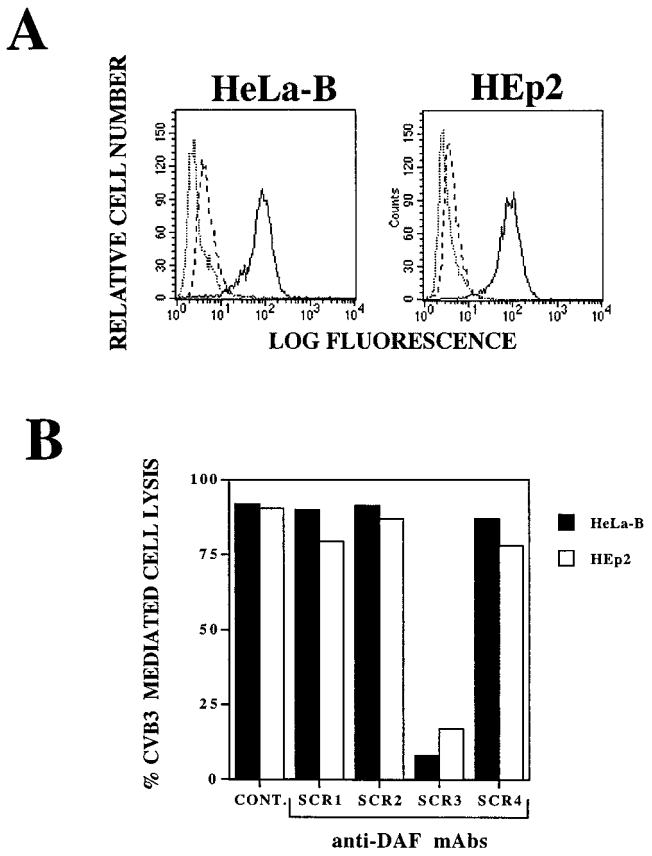

FIG. 3. MAb binding and blockade of CVB3 lytic infection in HeLa-B and HEp-2 cells. (A) Flow cytometric analysis of anti-DAF MAb (IH4) and anti-CAR MAb (RmcB) binding to HeLa-B and HEp-2 cells. The dotted histogram represents binding of the anti-mouse conjugate, the dashed histogram represents binding of the anti-CAR MAb, and the solid histogram represents binding of the anti-DAF MAb. (B) Anti-DAF MAb blockade of CVB3 Nancy/New replication in HeLa-B and HEp-2 cells. Confluent 96-well monolayers of HeLa-B and HEp-2 cells were incubated with 50 μl (20 μg/ml) of a control (CONT.) MAb (anti-PTA-1) and anti-DAF MAb IA10 (SCR1), 5B2 (SCR2), IH4 (SCR3), or IIH6 (SCR4) for 1 h at 37°C prior to challenge with 100 μl of CVB3 Nancy/New per well (10^3 PFU). Following incubation for 48 h at 37°C, cell monolayers were stained with a crystal violet-methanol solution, and cell survival was quantitated by measuring the absorbance at 540 nm on a multiscan enzyme-linked immunosorbent assay plate reader (Flow Laboratories). Results are expressed as mean percentage of cell lysis relative to the uninfected control cell monolayers of duplicate wells.

Similar patterns of results were obtained following the examination of the binding of CVB3 Nancy/New to HEp-2 cells which had surface-expressed DAF removed with phosphatidylinositol-specific phospholipase C (PI-PLC). In these experiments, the PI-PLC-treated cells bound only 10% of the labeled CVB3 bound by untreated cells. Similarly, MAb blockade with the anti-CAR antibody reduced viral binding by 60% whereas the combined treatment of PI-PLC plus anti-CAR MAb abrogated viral binding (data not shown). These findings confirm the involvement of both DAF and CAR in CVB3 binding and infection.

CAR-expressing RD (RD-I) cells are susceptible to CVB3 infection. An unexpected finding that emerged during the course of this study was that RD cells which had undergone

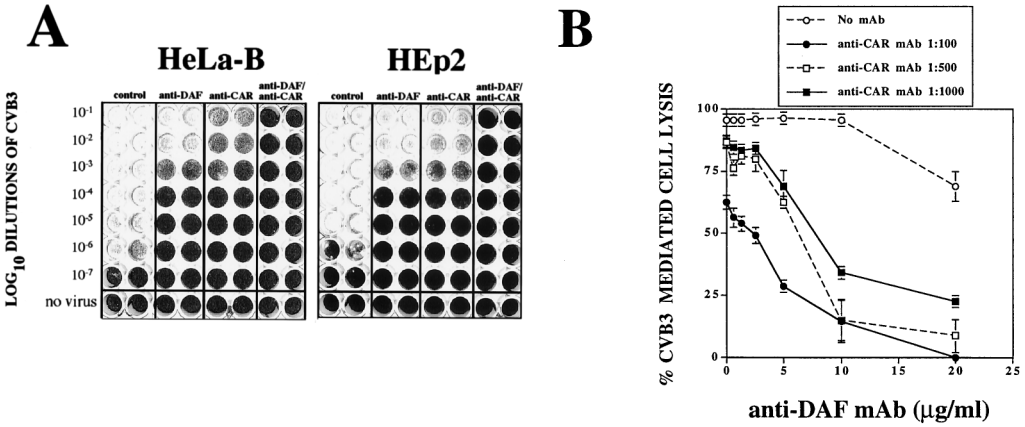

FIG. 4. Dose-dependent MAb blockade of CVB3 infection of HeLa-B cells. (A) To assess MAb blockade of virus-mediated cell lysis to a range of input multiplicities of CVB3 Nancy/New, cell monolayers in 96-well plates were incubated with 50 μl of anti-DAF (IH4) or control (anti-PTA-1) MAb (20 μg/ml) or anti-CAR (RmcB) MAb (1:100 dilution of ascites fluid) for 1 h at 37°C. Cell monolayers were then challenged with 100 μl of 10-fold serial dilutions of the stock CVB3 Nancy/New preparation (10^8 PFU/ml), and the plates were incubated at 37°C for 48 h, after which cell monolayers were stained with a crystal violet-methanol solution. (B) Monolayers of HeLa-B cells in 96-well plates were preincubated with the anti-DAF SCR3 MAb at concentrations from 0.625 to 20 μg/ml alone or in combination with anti-CAR MAb ascites at 1:100, 1:500, or 1:1,000 dilutions for 1 h prior to challenge with 10^5 PFU of CVB3 Nancy/New per well for 48 h at 37°C. To quantitate cell survival, monolayers were incubated with a crystal violet-methanol solution and washed with distilled water and the plates were read at a wavelength of 540 nm. Results are expressed as mean percentage of cell lysis relative to the uninfected control cell monolayers of triplicate wells ± standard deviations.

approximately 20 high-cell-density passages (RD-I cells) became susceptible to CVB3-mediated lytic infection. Flow cytometric analysis indicated that DAF expression was unchanged before and after high-density passage but that after 20 passages the RD-I cells had established a level of surface expression of CAR comparable to that on the surface of HeLa-B and HEp-2 cells (Fig. 5A). Immunoprecipitation with the anti-CAR MAb identified a polypeptide of approximately 47 kDa in lysates of surface biotinylated HEp-2, HeLa-B, and RD-I cells (data not shown). MAb blockade studies involving pretreatment with the anti-CAR MAb totally protected RD-I cells from lytic infection by 10^6 PFU of CVB3/well, while with these cells, anti-DAF MAb blockade had little inhibitory effect on any amount of virus (Fig. 5B).

In this study we have attempted to clarify the events involved in the cell attachment and entry mechanism of a DAF-binding strain of CVB3. It is postulated that while all strains of CVB3 are likely to bind to CAR, the presence of amino acids Val 108 and Ser 151 in the capsid protein VP2 of some CVB3 isolates correlates with an additional DAF-binding phenotype. However, the presence of these residues alone is insufficient to mediate lytic infection following DAF binding and hence does not confer an RD-positive phenotype on the virus. This observation confirms the report (19) that a noncardiovirulent isolate of CVB3 possessing both of the above-mentioned residues did not infect RD cells. Clearly, the RD variant of CVB3 (9), which lytically infects RD cells, in the absence of CAR expression must utilize additional viral capsid epitopes to facilitate usage of DAF as a functional receptor. From examination of the amino acid differences between the strains listed in Table 2, it appears that two such potential residues may be Leu 137 and Val 155 in VP3, and it is postulated that mutation of Pro 137 to Leu and/or Ile 155 to Val may confer the RD-positive phenotype on CVB3 Nancy/New. Investigations into these matters are currently under way.

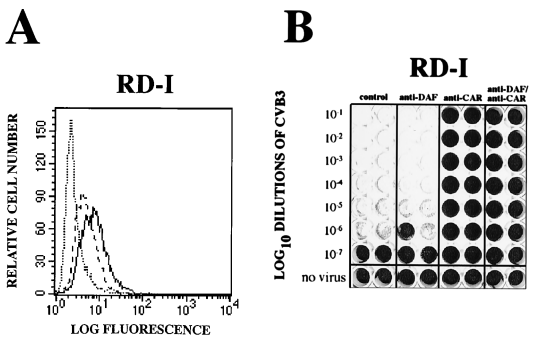

FIG. 5. MAb binding and blockade of CVB3 lytic infection in RD-I cells. (A) Flow cytometric analysis of anti-DAF MAb (IH4) and anti-CAR MAb (RmcB) binding to RD-I cells. The dotted histogram represents binding of the anti-mouse conjugate, the dashed histogram represents binding of the anti-CAR MAb, and the closed histogram represents binding of the anti-DAF MAb. (B) To assess MAb blockade of virus-mediated cell lysis to a range of input multiplicities of CVB3 Nancy/New, RD-I cell monolayers in 96-well plates were processed as described in the legend to Fig. 4.

CVB3 Nancy/New is a DAF-binding strain, but it requires CAR to effect cell entry, as shown by antibody blockade with anti-DAF and anti-CAR MAbs and by the failure of the virus to infect RD cells until these cells acquired CAR expression. CVB3 Nancy/New infectivity of the resultant RD-I cells was totally inhibited by the anti-CAR MAb alone. With the CVB3-permissive cell lines HeLa-B and HEp-2, which express both DAF and CAR, antibody-mediated blockade showed that the presence of MAbs to both DAF and CAR was required to effect total inhibition of lytic infection. This difference may be explained by the relatively much higher levels of DAF expressed by the HeLa-B and HEp-2 cells than by the RD cells, which may indirectly impede the binding efficiency of the anti-CAR MAb. This high level of DAF expression by these cells may also be invoked to suggest that the inhibition caused by the anti-DAF MAb may be the result of steric hindrance, if DAF is in close spatial association with CAR. Such a spatial relationship might be predicted, since chemical cross-linking studies have shown recently that DAF and ICAM-1 (another immunoglobulin superfamily member), which together form the receptor complex for coxsackievirus A21 (CVA21), are in a close spatial association (25). However, our finding that the removal of DAF from the HEp-2 cells with PI-PLC resulted in a loss of viral binding equivalent to that caused by anti-DAF

antibody blockade militates against steric hindrance being the cause of the inhibition.

It will be instructive to determine whether virus binding to DAF is sufficient to induce the conformational changes to the capsid proteins that are necessary to permit cell entry (5, 8, 11). Our results showing that the DAF-expressing RD cells do not permit viral lytic infection unless CAR is coexpressed implicate CAR binding as the crucial step in determining this process. In contrast, the CVB3 RD variant maybe conformationally altered following direct DAF interactions, permitting infection of DAF-positive, CAR-negative RD cells. The receptor-mediated entry of CVB3 may therefore be analogous to that of CVA21, which also binds to DAF but undergoes a conformational change to capsid proteins upon binding to ICAM-1 (24). What, therefore, is the physiological function of the DAF receptor for CVA21 and CVB3 if DAF is unable to induce capsid conformational changes? We propose that DAF may function as CVA21 and CVB3 sequestration sites, enhancing viral presentation to the functional ICAM-1 and CAR proteins. The potential of DAF to sequester CVB3 in a conformationally unaltered state may provide an explanation for an apparent discrepancy between data generated in this study and in that of Bergelson et al. (4) concerning the ability of anti-CAR MAb blockade to inhibit lytic infection of HeLa cells by DAF-binding CVB3 isolates. In the latter study (4) excess anti-CAR MAb was removed prior to viral challenge, leaving DAF-bound CVB3 free to interact with newly surface-expressed CAR and to initiate infection throughout the course of the viral plaque assay (24 to 72 h), thus bypassing the initial anti-CAR MAb treatment. However, in the present study excess anti-CAR MAb remained present throughout viral challenge and the infectivity assay incubation period of 48 h, thereby competing with CVB3 for newly expressed CAR and subsequently mediating inhibition of CVB3 lytic infection (Fig. 4A).

A possible additional role for DAF may be as a stabilizing receptor: binding to DAF may slow down the virus for interaction with the functional protein. This would be of advantage for efficient viral infection of cells surrounded by fluids with flow, i.e., blood and gastric and respiratory secretions. In support of this, it is interesting to note that low-passage clinical isolates of CVB3 bind to DAF on the surface of transfected cells and their DAF-binding phenotype is not acquired from passage in cell cultures (4). It is suggested that the differing affinities of individual CVB3 isolates for interaction with DAF and CAR may be major determinants in their tissue tropism and virulence. In addition to this, our checkerboard studies of antibody blockade showed evidence of lateral cooperativity between the DAF and CAR receptors, and it may be postulated that DAF also functions as a scaffold to position CAR for more effective viral binding.

We thank Richard Crowell and Jeffrey Bergelson for the anti-CAR MAb (RmcB), Taroh Kinoshita and Bruce Loveland for the anti-DAF MAbs, Gordon Burns for the anti-PTA-1 MAb, Reinhard Kandolf and Hans-Christoph Selinka for pCB3/T7, Margery Kennett for the echovirus 7 and CVB3 stock viruses, and Dale Levitzke of the Newcastle Biomolecular Research Facility for DNA sequencing.

This research was supported by a project grant from the National Health and Medical Research Council of Australia.

REFERENCES

1. **Bergelson, J. M., B. M. Chan, K. R. Solomon, J. N. St. John, and R. W. Finberg.** 1994. Decay-accelerating factor (CD55), a glycosylphosphatidylinositol-anchored complement regulatory protein, is a receptor for several echoviruses. Proc. Natl. Acad. Sci. USA **91:**6245–6249.
2. **Bergelson, J. M., J. G. Mohanty, R. L. Crowell, N. F. St. John, D. M. Lublin, and R. W. Finberg.** 1995. Coxsackievirus B3 adapted to growth in RD cells binds to decay-accelerating factor (CD55). J. Virol. **69:**1903–1906.
3. **Bergelson, J. M., J. A. Cunningham, G. Droguett, E. A. Kurt-Jones, A. Krithivas, J. S. Hong, M. S. Horwitz, R. C. Crowell, and R. W. Finberg.** 1997. Isolation of a common receptor for coxsackie B viruses and adenoviruses 2 and 5. Science **275:**1320–1323.
4. **Bergelson, J. M., J. F. Modlin, W. Wieland-Alter, J. A. Cunningham, R. C. Crowell, and R. W. Finberg.** 1997. Clinical coxsackievirus B isolates differ from laboratory strains in their interaction with two cell surface receptors. J. Infect. Dis. **175:**697–700.
5. **Casasnovas, J. M., and T. M. Springer.** 1994. Pathway of rhinovirus disruption by soluble intercellular adhesion molecule 1 (ICAM-1): an intermediator in which ICAM-1 is bound and RNA is released. J. Virol. **68:**5882–5889.
6. **Clarkson, N. A., R. Kaufman, D. M. Lublin, T. Ward, P. A. Pipkin, P. D. Minor, D. J. Evans, and J. W. Almond.** 1995. Characterization of the echovirus 7 receptor: domains of CD55 critical for virus binding. J. Virol. **69:**5497–5501.
7. **Coyne, K. E., S. E. Hall, E. S. Thompson, M. A. Arce, T. Kinoshita, T. Fujita, D. J. Anstee, W. Rosse, and D. M. Lublin.** 1992. Mapping of epitopes, glycosylation sites, and complement regulatory domains in human decay accelerating factor. J. Immunol. **149:**2906–2913.
8. **Crowell, R. L., and L. Philipson.** 1971. Specific alteration of coxsackievirus B3 eluted from HeLa cells. J. Virol. **8:**509–515.
9. **Crowell, R. L., A. K. Field, W. A. Schleif, W. L. Long, R. J. Colonno, J. E. Mapoles, and E. A. Emini.** 1986. Monoclonal antibody that inhibits infection of HeLa and rhabdomyosarcoma cells by selected enteroviruses through receptor blockade. J. Virol. **57:**438–445.
10. **de Verdugo, U. R., H.-C. Selinka, M. Huber, B. Kramer, J. Kellermann, P. H. Hofschneider, and R. Kandolf.** 1995. Characterization of a 100-kilodalton binding protein for the six serotypes of coxsackie B viruses. J. Virol. **69:**6751–6757.
11. **Gomez Yafal, A., G. Kaplan, V. R. Racaniello, and J. M. Hogle.** 1993. Characterization of poliovirus conformational alteration mediated by soluble cell receptors. Virology **197:**501–505.
12. **Hsu, K.-H. L., K. Lonberg-Holm, B. Alstein, and R. L. Crowell.** 1988. A monoclonal antibody specific for the cellular receptor for the group B coxsackieviruses. J. Virol. **62:**1647–1652.
13. **Kinoshita, T., M. E. Medof, R. Silber, and V. Nussenzweig.** 1985. Distribution of decay accelerating factor in the peripheral blood of normal individuals and patients with paroxysmal nocturnal hemoglobinuria. J. Exp. Med. **162:**75.
14. **Klump, W. M., I. Bergmann, B. C. Müller, D. Ameis, and R. Kandolf.** 1990. Complete nucleotide sequence of infectious coxsackievirus B3 cDNA: two initial 5′ uridine residues are regained during plus-strand RNA synthesis. J. Virol. **64:**1573–1583.
15. **Knowlton, K. U., E.-S. Jeon, N. Berkley, R. Wessely, and S. Huber.** 1996. A mutation in the puff region of VP2 attenuates the myocarditic phenotype of an infectious cDNA of the Woodruff variant of coxsackievirus B3. J. Virol. **70:**7811–7818.
16. **Lindberg, A. M., P. O. K. Stalhandske, and U. Petterson.** 1987. Genome of coxsackievirus B3. Virology **156:**50–63.
17. **Lindberg, A. M., R. L. Crowell, R. Zell, R. Kandolf, and U. Petterson.** 1992. Mapping the RD phenotype of the Nancy strain of coxsackievirus B3. Virus Res. **24:**187–196.
18. **Lonberg-Holm, K., R. L. Crowell, and L. Philipson.** 1976. Unrelated animal viruses share receptors. Nature (London) **259:**679–681.
19. **Muckelbauer, J. K., M. Kremer, I. Minor, G. Diana, F. J. Dutko, J. Groarke, P. C. Pevear, and M. G. Rossmann.** 1995. The structure of coxsackievirus B3 at 3.5A resolution. Structure **3:**653–667.
20. **Nicholson-Weller, A., and C. E. Wang.** 1994. Structure and function of decay accelerating factor CD55. J. Lab. Clin. Med. **123:**485–491.
21. **Reagan, K. J., B. Goldberg, and R. L. Crowell.** 1984. Altered receptor specificity of coxsackievirus B3 after growth in rhadomyosarcoma cells. J. Virol. **49:**635–640.
22. **Schmidt, N. J., H. H. Ho, and E. H. Lennette.** 1975. Propagation and isolation of group A coxsackieviruses in RD cells. J. Clin. Microbiol. **2:**183–185.
23. **Shafren, D. R., R. C. Bates, M. V. Agrez, R. L. Herd, G. F. Burns, and R. D. Barry.** 1995. Coxsackieviruses B1, B3, and B5 use decay accelerating factor as a receptor for cell attachment. J. Virol. **69:**3873–3877.
24. **Shafren, D. R., D. J. Dorahy, S. J. Greive, G. F. Burns, and R. D. Barry.** 1997. Mouse cells expressing human intercellular adhesion molecule-1 are susceptible to infection by coxsackievirus A21. J. Virol. **71:**785–789.
25. **Shafren, D. R., D. J. Dorahy, R. A. Ingham, G. F. Burns, and R. D. Barry.** 1997. Coxsackievirus A21 binds to decay accelerating factor but requires intercellular adhesion molecule-1 for cell entry. J. Virol. **71:**4736–4743.
26. **Tomko, R. P., R. Xu, and L. Philipson.** 1997. HCAR and MCAR: the human and mouse cellular receptors for subgroup C adenoviruses and group B coxsackieviruses. Proc. Natl. Acad. Sci. USA **94:**3352–3356.
27. **Vuorinen, T., R. Vainionpää, R. Vanharanta, and T. Hyypiä.** 1996. Susceptibility of human bone marrow cells and hematopoietic cell lines to coxsackievirus B3 infection. J. Virol. **70:**9018–9023.
28. **Ward, T., P. A. Pipkin, N. A. Clarkson, D. M. Stone, P. D. Minor, and J. W. Almond.** 1994. Decay accelerating factor CD55 is identified as the receptor for echovirus 7 using CELICS, a rapid immuno-focal cloning method. EMBO J. **13:**5070–5074.